Soong *et al. Chem. Biol. Technol. Agric.* (2017) 4:3
DOI 10.1186/s40538-016-0084-2

Chemical and Biological Technologies in Agriculture

RESEARCH Open Access

Water-mediated NOE: a promising tool for interrogating interfacial clay–xenobiotic interactions

Ronald Soong, Adolfo Botana, Jasmine Wang, Hashim Farooq, Denis Courtier-Murias and Andre Simpson*

Abstract

Background: The sorption of anthropogenic compounds on clay minerals is a complex molecular process with important implications for the fate of agrochemicals and organic pollutants in the environment.

Results: The present study illustrates the use of a water-mediated NOE approach to study clay binding interactions. This method exploits the interfacial water layer on clay surfaces as a hydrogen reservoir for magnetization transfer. The interactions of four different xenobiotics with clay suspension were investigated through this method to demonstrate its capability to screen for the clay–xenobiotic molecular affinity. Further, based onthe NOE build-up rates, epitope map of clay–xenobiotic interactions can be generated, explaining theorientation and mechanism of the interactions.

Conclusions: The water-mediated NOE approach has the potential to reveal key insights into the role that interfacial water plays in the binding process, providing a better understanding of the partitioning of anthropogenic compounds from bulk water into aqueous clay suspensions.

Background

The enormous number of different xenobiotic substances in our environment is becoming a significant health concern [1–3]. These xenobiotic substances, including hormones, antibiotics and numerous pesticides, are commonly released to the environment through human activities [2–4]. As these substances accumulate in our environment, the question of their bioavailability becomes increasingly important. For instance, the occurrence of hormones, particularly estrogens, has recently gained attention due to their toxicological significance and their influence on biological activities in aquatic organisms [2, 4]. Although the acute health effects of these xenobiotics are well documented, the effect of chronic exposure remains an open question [1–3, 5, 6]. The intrinsic interactions between these xenobiotics and soils hold the key to understanding both their environmental accumulation and their bioavailability [7–11]. Therefore, a better understanding as to how xenobiotics are sequestered into complex rock, soil, and sediments is required [12–14].

Soil is represented by a complex mixture consisting of mineral and organic constituents that are in solid, gaseous, and aqueous states [15]. Amongst the inorganic constituents in soil, clays constitute the major component (often around 30% w/w) and are important in the preservation of labile organic compounds. Clays are inorganic materials composed prevalently of layers of SiO_4 and/or AlO_4 [16]. Because of their anionic nature, the surfaces of clays are covered with small cations. For instance, a host of cations, such as Na^+, Ca^{2+}, Mg^{2+}, K^+, and NH_4^+ are capable of binding to clay surfaces, giving them different colloidal property [16]. In addition to sequestering cations from solution, clays are capable of adsorbing water molecules on their surfaces through hydrogen bonding, allowing them to expand and swell several times their dry mass [17, 18]. Due to this excellent colloidal property, clay is often been employed in a range of applications, from mining to agriculture [19].

So far, most soil–organic interaction studies mainly concerned the association of xenobiotic with humic substances [13, 20, 21]. These studies reveal that the

*Correspondence: andre.simpson@utoronto.ca
Environmental NMR Center, University of Toronto Scarborough, 1265 Military Trails, Toronto, ON M1C 1A4, Canada

xenobiotics are sequestered into soils through weak interactions driven synergistically by both hydrophobic and hydrophilic interactions [21]. Despite the inorganic nature of clay, it is able to interact with a number of organic molecules such as fatty acids and aromatic compounds [22, 23]. In addition, recent studies have demonstrated that soluble organic matters (SOM) from terrestrial source are able to bind to clay particles in solution [12, 13]. Although the binding between clay and organic matter has already been demonstrated, the exact mechanism of interactions at the interface remains an open question due to the lack of suitable high-resolution structure determination techniques. Since these organic compounds exhibit a range of binding affinity to clay particles, traditional high-resolution diffraction techniques, such as SANS and powder XRD, are ill-suited to tackle such problems [19, 24]. In fact, this requires a technique that can interrogate molecular interactions over a wide range of timescales.

Nuclear magnetic resonance (NMR) spectroscopy has evolved into an indispensable technique capable of providing insights into different intermolecular interactions over a range of time scales (ms to ns) as shown in Fig. 1 [14, 20, 25–28]. For a complete review of NMR techniques and applications to understand interactions in environmental samples, readers should refer to an excellent review by Mazzei and Piccolo [28]. In environmental research, NMR is becoming an important tool used to highlight specific interactions between different constituents in soils [21, 29–32]. Over the years, numerous detailed NMR studies have provided valuable information on the underlying factors regarding the different binding properties of a number of anthropogenic contaminants [31–35]. Recently, a novel NMR technology was introduced, termed as comprehensive multiphase (CMP) NMR [38]. This approach combines hardware from solution, gel, and solid-state NMR into a single probe and permits environmental samples to be investigated in situ, in their fully hydrated state, and in all phases, allowing for all phases to be simultaneously investigated [28, 35–38]. A number of NMR techniques can be used to investigate interactions between organic soil constituents [31, 36, 39]. A brief summary illustrating the different NMR techniques and the length/time scales of interaction is shown in Fig. 1. Most of these techniques are based on the transfer of magnetization through physical interactions and result in a detectable NMR signal. The magnitude of this magnetization transfer is proportional to the strength of the interactions involved. Therefore, NMR becomes the tool of choice to unravel the complexity behind various intermolecular interactions. Amongst these experiments, magnetization transfer through nuclear overhauser effects (NOE) and saturation transfer difference (STD) are commonly used to determine intermolecular interactions [31, 39–41]. For most NMR experiments, magnetization transfer requires the ability to saturate an observable NMR signal. Commonly this involves interactions between one organic material (for example soil organic matter) and an organic ligand (for example a contaminant). However, in the case of minerals and clays, which do not contain an organic phase, this can be more challenging.

NMR has been successfully applied in investigating clay–organic exposure in recent studies [21, 42]. Most of these studies often involved solid-state NMR (SSNMR) techniques with compounds irreversibly bound on clay surfaces [21, 43, 44]. For instance, ^{29}Si NMR combined with cross polarization (^{1}H–^{29}Si) under magic angle spinning (CP-MAS) was used to investigate the binding of

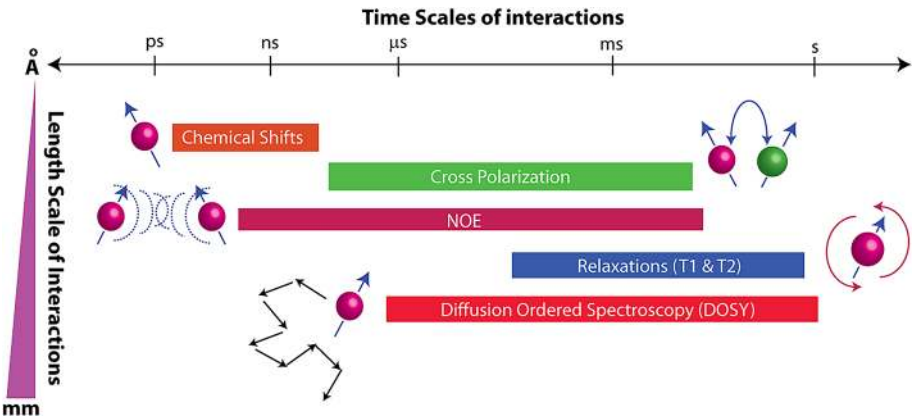

Fig. 1 An illustration of NMR observable parameters/experiments and their associated time/length scale dependence. According to this figure, NMR is able to probe a wide range of interactions over a range of time/length scales. Importantly, in environmental science, a range of interactions exists in soil such that a single NMR experiments will yield only a piece of the puzzle. Therefore, in order to fully understand the dynamics of the system, it is important to perform a range of different NMR experiments, allowing for a better view of the system involved

chemicals on clay surfaces [42–44]. Importantly, SSNMR techniques require that molecules to be bound tightly on the surface and the samples have to be dry. However, less information is available with regards to fully hydrated clay and dynamic interactions. To help bridge this gap in our understanding of clay–organic interactions, water-mediated nuclear overhauser effect (NOE) will be investigated in this study. Owing to the hydration layers on clay surfaces [18, 45], intermolecular NOE from the clay–bound water can be transferred to other molecules if they are in contact with each other, allowing their interactions at the atomistic level to be probed. In addition, ^{1}H-^{1}H NOE can be a sensitive technique used to probe weak intermolecular interactions [46]. A diagrammatic representation of a hydrated clay–organic system is shown in Fig. 2. In the present study, we demonstrate the avenue in which water-mediated NOE can be transferred to a clay–bound molecules via an NMR radio frequency (r.f.) sequence called Water Ligand Observed via Gradient Spectroscopy (waterLOGSY) [40, 47, 48]. In order to illustrate the usefulness of this sequence, a series of xenobiotic compounds will be screened for their affinity for clay particles, allowing us to evaluate its effectiveness in organo-clay research.

Methods

Materials

All chemicals, including pesticides, were purchased from Sigma-Aldrich. The mica-montmorillonite was purchased from the Clay society (www.clay.org). The montmorillonite was carefully treated according to the procedure outlined in the subsequent section before use.

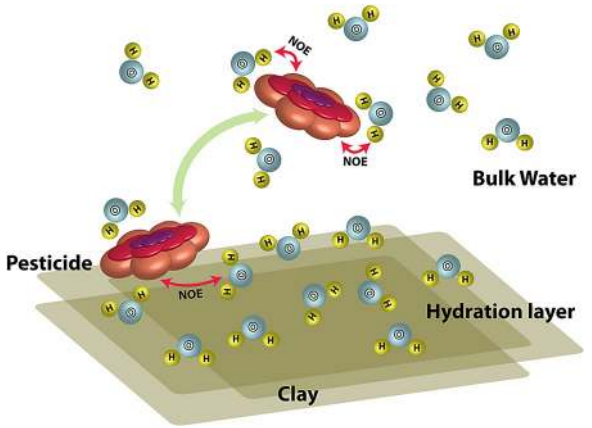

Fig. 2 An illustration of the interaction between pesticides and water on clay surface. In this case, we have two different types of water molecules with different dynamics. Due to the oxygen-rich surface, the clay surface is covered with water due to hydrogen bonding. The clay–bound water exhibits correlation time that is significantly lower compared to that of free water, leading to a different sign in their NOE. If the pesticide is in contact with the water molecules, magnetization from the water will be transferred to the pesticides via NOE

Preparation of colloidal clay particles

Synthetic mica-montmorillonite (<2 μm, NL Industries) was subject to sodium exchange and saturation in order to form a stable suspension. A centrifuge tube was filled to approximately 1.5 cm with clay, and to 8 cm with 1 M sodium chloride solution. The centrifuge tube was continuously inverted until the clay was thoroughly suspended. The mixture was centrifuged for 5 min at 2000 rpm. The supernatant was decanted, and the procedures stated above were repeated two additional times. After the last decantation, the centrifuge tube was filled to 8 cm with distilled water and the clay was re-suspended. This mixture was centrifuged for 5 min at 2000 rpm. The supernatant was decanted, and the distilled water wash was repeated two more times in order to obtain a supernatant which appeared turbid. The Na-saturated sediment was then re-suspended in distilled water and two drops of 5 M sodium chloride solution. The mixture was centrifuged for 6 min at 1000 rpm. The turbid supernatant was pipetted into a 500-mL beaker with caution to prevent disturbing the sediment. This process was repeated seven more times until the supernatant was clear. The bulk supernatant containing Na-saturated clay was freeze dried.

Preparation of NMR samples

5 mg of pesticide and 10 mg of colloidal clay were dissolved in 500 μL of H_2O/D_2O (90:10). The mixture was stirred on a vortexer for 30 min and was subsequently transferred to a 5-mm NMR tube. The pH of the solution was tested via litmus paper.

NMR spectroscopy

The NMR experiments were acquired on a Bruker Avance III NMR spectrometer operating at 11.7 T, observing ^{1}H at 499.98 MHz. The ^{1}H field strength used was 25 kHz, with an acquisition length of 4 k data points and 15 ppm spectral width. The ^{1}H waterLOGSY spectra were averaged over 128 scans with a recycle delay of 5 s. All NMR spectra were recorded at 297 K using a 4-channel 5-mm QXI inverse detection probe tuned to ^{1}H, ^{13}C, ^{15}N, and ^{19}F. Typical parameters used for waterLOGSY experiment were as follows: 4-ms 180° selective pulse (Φ_2) with Gaussian shape along with a 5-ms sinc-shaped 90° pulse (Φ_5) (water flipback) were used for selecting the water resonance; 1 ms squared gradient pairs were used at 40% of the maximum gradient strength (~54 G/cm) to select the water signal; and 2-ms square pulses (Φ_6 and Φ_8) along with gradients at 31 and 11% to dephase the water during water suppression. A gradient at 0.2% was applied

throughout the mixing time to dephase water magnetization. A gradient recovery of 200 µs was used. The typical mixing times used in the waterLOGSY experiments were between 10 ms to 1.5 s. The mixing times used should be less than or equal to that of the longitudinal (T_1) of water.

Data processing

The NMR spectra were processed by applying an exponential multiplication of the FIDs by a factor of 5 Hz prior to Fourier transform and zero filled to 8 K. The waterLOGSY NOE build-up curve was fitted according to the following equation and assumed to be a two-spin model for which the NOE intensity is given by [49]

$$\eta = \frac{\sigma}{\rho}[1 - \exp(-\rho t)] \quad (1)$$

where σ is the cross-relaxation rate, ρ is the spin lattice relaxation rate, and t is the mixing time. The epitope maps based on NOE build-up (Fig. 9) were generated through measuring the changes in the cross-relaxation rate in either the presence or the absence of suspended clay particles for each resolvable ^{1}H resonances in the NMR spectrum. The epitope maps calculated from a single mixing time are simply derived from the relative change in signal intensity on addition of clay. In both cases, the position showing the strongest interaction (highest peak) is set to 100%, whereas the other hydrogens are progressively scaled accordingly.

Discussion

Numerical simulation of NOE based on clay–bound interactions

WaterLOGSY is a commonly used radio frequency (r.f.) NMR sequence for screening ligand–protein interactions [40, 41, 47, 48]. The pulse sequence is shown in Fig. 3. This sequence was conceived to exploit the differences in the dynamics between bound water on protein surfaces and free water in solution. When water molecules are bound on a protein, their correlation times will increase temporarily to match that of the protein, thus leading to a change in the sign of their NOE [40, 47, 48]. Similarly, for the case of clay–bound water molecules, the sign of their NOE will be opposite of that in free water due to the differences in their correlation times. Unlike proteins, the water molecules on clay surface are tightly bound such that a constant hydrogen reservoir can be assumed to be available for NOE transfer [45, 50]. Therefore, in this case, we can assume that for NOE transfer to occur, the residence time of the xenobiotics on clay surface will be comparable to that of clay–bound water. In this case, the relationship between the rate of NOE transfer between xenobiotics and clay–bound water can be described via Eq. (2) [40, 47, 48]

$$\sigma_{wc} = \frac{\gamma^4 \hbar^2 \left(\frac{\mu_o}{4\pi}\right)}{10 r^6} \left(\frac{\tau_r \tau_p}{\tau_r + \tau_p}\right) \left(\frac{6}{1 + \frac{4\omega_0^2 (\tau_r \tau_p)^2}{(\tau_r + \tau_p)^2}} - 1\right), \quad (2)$$

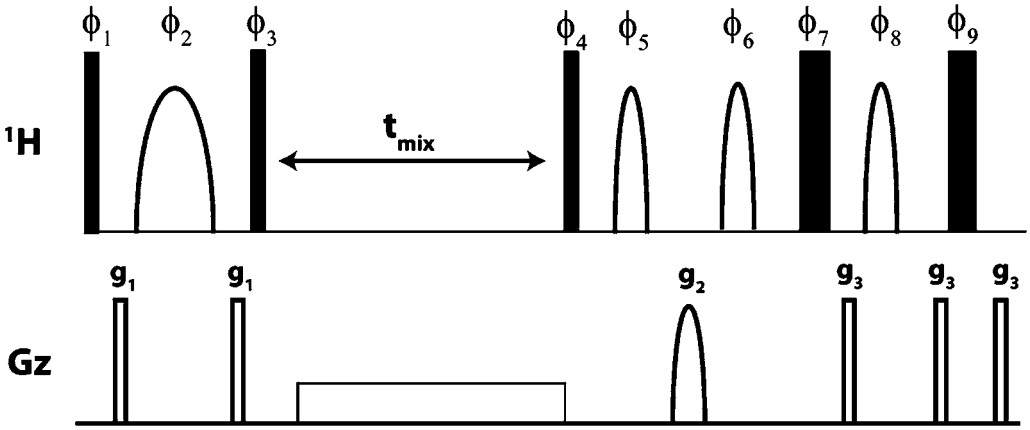

Fig. 3 A schematic illustrating the radio frequency (r.f.) pulse sequence used for a homonuclear one-dimensional WaterLOGSY experiment. A 180° Gaussian shape pulse (Φ_2), in combination with a gradient (g_1), is used to select for the water signal. During the mixing time (t_{mix}), the NOE from the water is transferred to a molecule only if they are in contact with each other. A small continuous gradient is applied during t_{mix} to reduce the effect of radiation damping. Lastly, both water flipback [5-ms sinc-shaped 90° pulse (Φ_5)] and excitation sculpting (Φ_6 and Φ_8) are used for water suppression before signal acquisition. (*Note* The pulse length for excitation sculpting was calibrated to achieve optimal water suppression) The phase cycling for each pulse is as followed: $\Phi_1 = 0$, $\Phi_2 = 0123$, $\Phi_3 = (0)_4\,(2)_4$, $\Phi_4 = 0$, $\Phi_5 = 02$, $\Phi_6 = (2)_8(3)_8(2)_8(3)_8(0)_8(1)_8(0)_8(1)_8$, $\Phi_7 = (0)_8(1)_8(0)_8(1)_8(2)_8(3)_8(2)_8(3)_8$, $\Phi_8 = (2)_4(3)_4(2)_4(3)_4(0)_4(1)_4(0)_4(1)_4$, $\Phi_9 = (0)_4(1)_4(0)_4(1)_4(2)_4(3)_4(2)_4(3)_4$, and $\Phi_{rec} = 0123012323012301$. The gradient amplitudes (%) were set to 40, 31, and 11 for g_1, g_2, and g_3, respectively. The phase cycle requires at least two transients

where γ is the gyromagnetic ratio of hydrogen nuclei, $\hbar$ is Planck's constant divided by 2π, μ_0 is the permeability of free space, r is the distance between the observed ^{1}H on the molecules and water, τ_r is the residence time of the molecules, τ_p is the rotation correlation times of the clay particles, and ω_0 is the Larmor frequency.

In order to understand the rate of NOE build-up in our system, a numerical simulation is performed. In this case, we assume the average clay particle to be 0.2 μm in diameter and are able to tumble freely in solution. Also, the water molecules are assumed to be tightly bound on the clay surface where they form a rich hydrogen reservoir, facilitating magnetization transfer via NOE. The result of the simulation was shown in Fig. 4. The simulation demonstrates the dependence of σ_{wc} on both r and τ_r. Our simulation illustrates that the effective distance on NOE build-up rate is limited to 2 Å. This is short compared to the typical 5 Å range for NOE, indicating that physical contact appears to be the primary mechanism for magnetization transfer. Interestingly, the sign of the NOE build-up is critically dependent on the residence time of the molecules on the clay surface. For short residence times, we observed a positive build-up rate which became negative as the residence time increased. The crossover point is ~2 ns residence time. Therefore, this demonstrates that a molecule's affinity for clay can be revealed via the sign of its NMR signals. From our simulation, we can conclude the following: (1) the magnetization transfer from clay–bound water can only occur through contact, (2) the sign of NOE build-up of the molecules that are in contact with clay–bound water will be opposite compared to those in contact with free water, (3) only if the residence time of the molecules on clay surface is greater than 2 ns, it is possible to observe a change in the sign of their NMR signals.

^{1}H waterLOGSY NMR spectra of four different xenobiotics in the absence and presence of clay particles

In order to demonstrate the applicability of waterLOGSY, three different pesticides were chosen, namely Diflufenzopyr, Imazapyr, and Nicotine. While Nicotine is most famous for being a key component of tobacco, it is now employed as a pesticide [51]. In addition, DMSO is employed as a control/reference as it is known to form hydrogen bonds with water and break/compete with hydrogen bonds occurring on clay surfaces [52]. Figure 5 shows the structural assignments for the xenobiotics used in this study. The observed ^{1}H chemical shifts values, and multiplet patterns are consistent with the literature values [12]. The xenobiotics used in this study contain different functional moieties that span most of

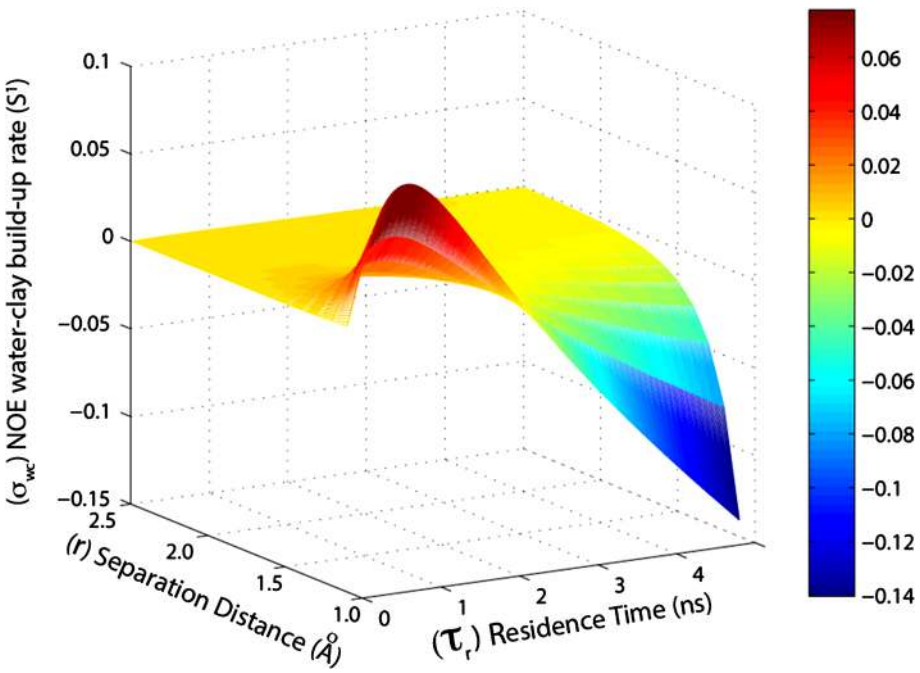

Fig. 4 A numerical simulation of the NOE water–clay build-up rate (σ_{wc}) as a function of both separation distance (r) and residence time (τ_r). This simulation illustrates that the sign of the NOE build-up rate depends on how long the molecules stay on the clay surface. In addition, NOE build-up occurs only within a separation distance of ≈2 Å, which is far less than the typical 5 Å range for NOE. The crossover point in which the build-up rate becomes negative is ~2 ns

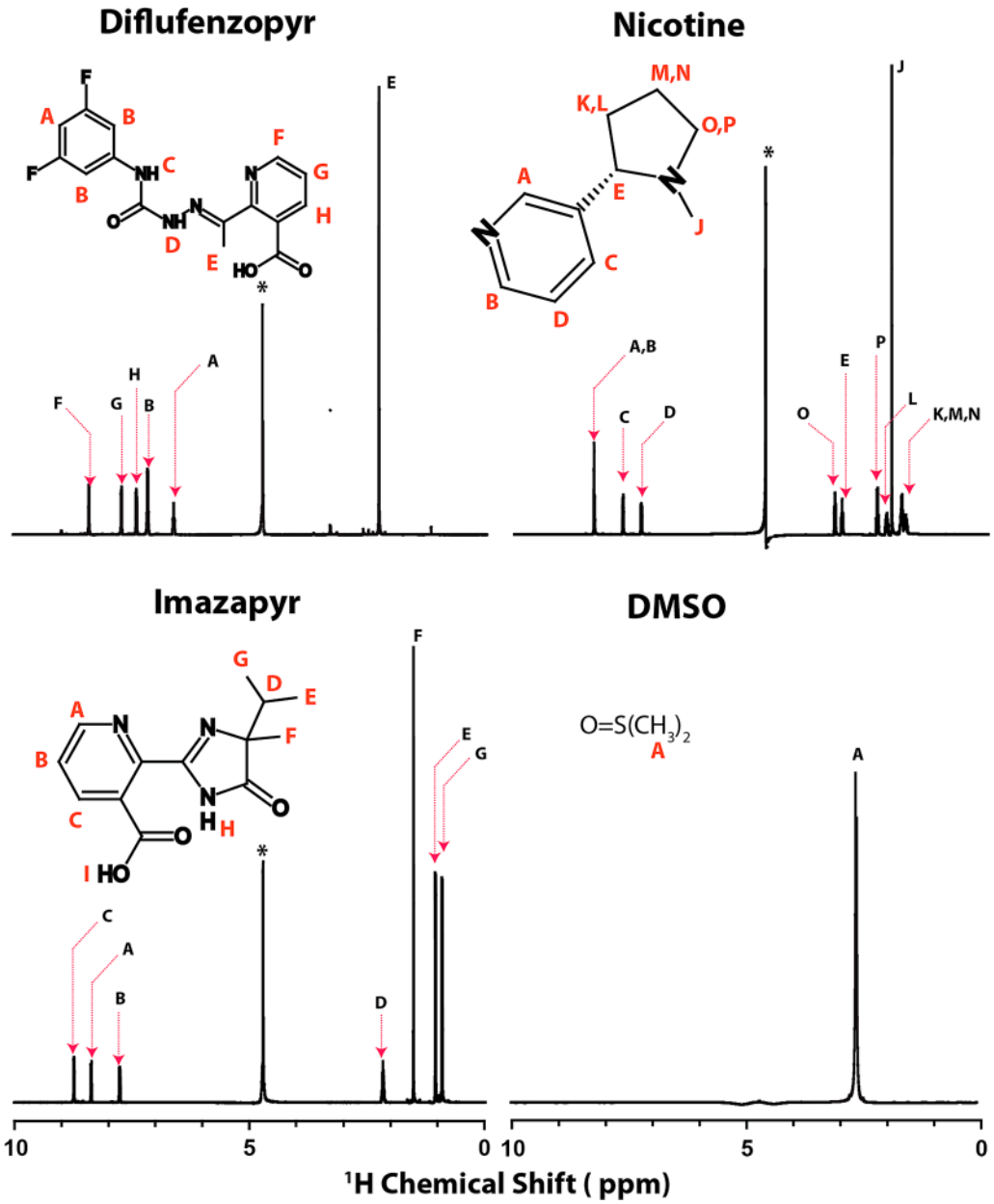

Fig. 5 ^{1}H NMR spectra of four different xenobiotics used in our current study. (*Note*: *Asterisk* denotes residual water)

the ^{1}H chemical shift range. These moieties can influence the manner in which molecules interact with clay surfaces. Importantly, the water-mediated NOE transfer may shed new insights into the parameters that dictate these interactions.

A series of waterLOGSY spectra was acquired for the four different xenobiotics, and it is shown in Fig. 6. These spectra were acquired in the presence and in the absence of clay in order to highlight changes in molecular interactions, which can be detected via waterLOGSY. The presence of clay particles indeed changes some of the ^{1}H spectral features of the xenobiotics in the current studies. For instance, a noticeable increase in ^{1}H resonance line width of Nicotine is observed in the presence of clays as shown in the loss of resolution in many of the multiplet patterns. The changes in the linewidth in some of the xenobiotics are an indication of interactions. Since linewidth can be a measure of mobility, this points to a situation in which the compound temporarily binds to the surface of the clay particles, resulting in an

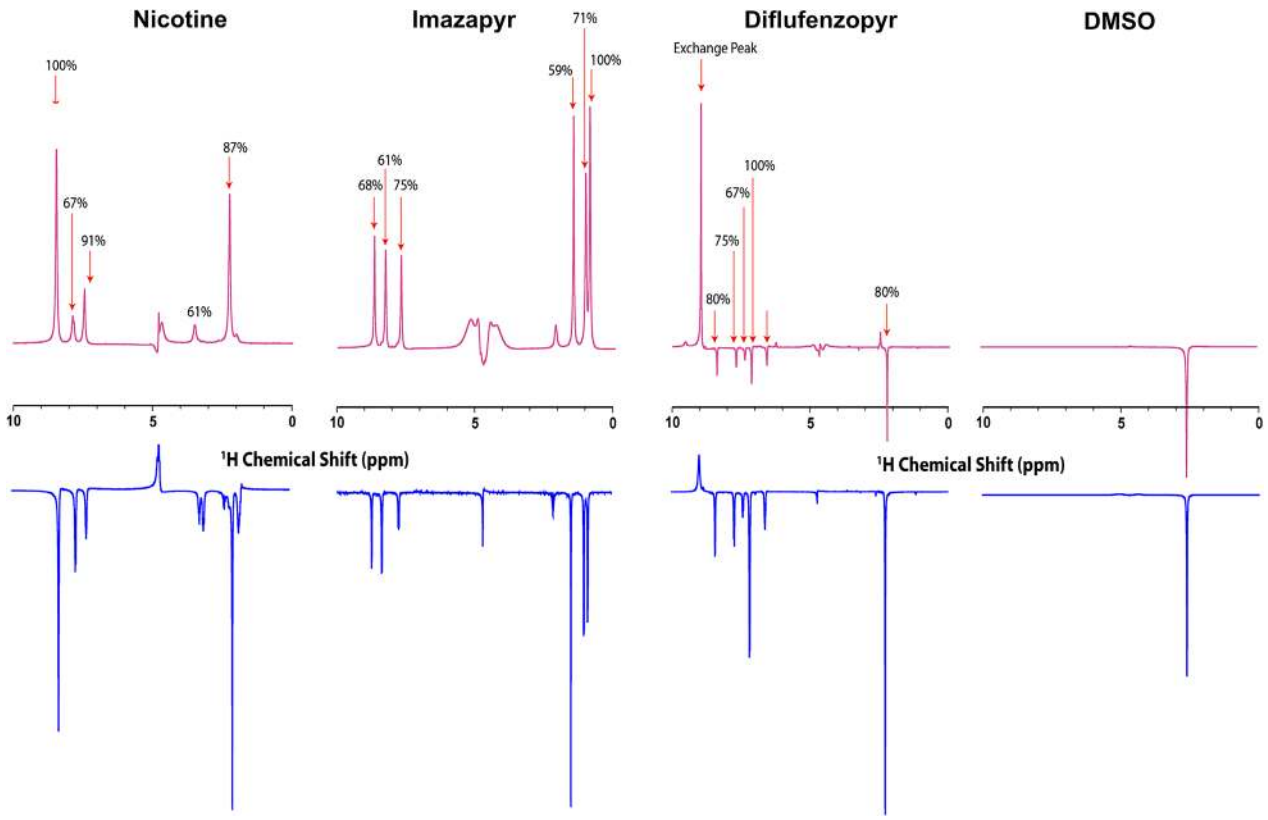

Fig. 6 ^{1}H NMR WaterLOGSY spectra of four different xenobiotics. The four different compounds used in this current study are Nicotine, Imazapyr, Diflufenzopyr, and dimethyl sulfoxide (DMSO). *Top* WaterLOGSY spectra in the presence of clay. *Bottom* WaterLOGSY spectra in the water. The mixing time used to acquire waterLOGSY spectra was 800 ms. The differences in the intensity between the spectra were attributed to the different NOE build-up rates

increase in their correlation times. Notwithstanding the changes in the linewidth, the resonances in these spectra remain resolved, except for peaks K, L, M, and N as well as O and E of Nicotine which overlapped with each other (Fig. 6). Based on these spectral features, the interactions between the molecules and clay particles are likely in the fast exchange regime where waterLOGSY would prove to be applicable. Another indication that the system is in a fast exchange region is the fact that we only observed a small shifts in all hydrogen resonances, indicating that the interactions were fast in the chemical shift timescale. (Note: if the system is undergoing a slow exchange, two resonances, bound and free, are observed.)

The changes in the sign of the NOE depending on clay's presence confirm that interactions occur for the case of Nicotine and Imazapyr. On the other hand, there is no change in the sign of the NOE for the case of Diflufenzopyr and DMSO; this indicates that their interactions with the clay particle were transient at best. Furthermore, the aromatic ^{1}H peaks of Diflufenzopyr remain inverted despite the absence of clay, while the amide proton (~9 ppm) has an opposite phase due to fast exchange. The different intensities for hydrogen in the NMR spectrum can be attributed to the clay interactions leading to differences in the NOE build-up rate and can be confirmed through experiments with varying mixing times. Epitope maps, which provide information on the binding orientation, can be generated from the data in Fig. 6 as well as from NOE build-up curves. Both these approaches are discussed later in the paper. In conclusion, the results of these experiments confirm our numerical simulations that indeed, clay–bound water-mediated NOE can be used to discriminate binding interactions on clay surfaces.

Strength of clay–bound interaction revealed through NOE build-up

The rate of NOE build-up can provide a qualitative measure on the strength of the interactions between clay particles and various xenobiotics. Since most of the clay particle sizes are in the range of microns, the key factor in determining the NOE build-up rate will be the residence time of a molecule on clay surfaces. In essence, the length of time a molecule spent on clay surfaces reflects

the strength of their interactions. A series of NOE build-up curves was collected (Fig. 7), and the build-up rates were extracted for each of the resolvable resonances. The build-up rates for each compound were summarized as in a bar graph in Fig. 8. An overall increase in the build-up rates was observed in the presence of clay irrespective of their affinity for clay surfaces. Importantly, this increase in the build-up rate can be attributed to their weak transient molecular interactions with clay particles. This is consistent with our simulation results that even at short residence time, an increase in the NOE build-up rate will be observed. However, only when the residence time exceeds 2 ns does a change in NOE build-up rate along with a change in the sign occur. For molecules showing an affinity for clay particles such as Nicotine and Imazapyr, we observed a significant increase in the NOE build-up rate. On the other hand, for DMSO and Diflufenzopyr where their interactions with clay surfaces are weak, we observed only a slight change in their respective NOE build-up rate. Interestingly, DMSO indiscriminately formed hydrogen bonds with water and most likely interacted with bulk water molecules. Thus, these experiments provide a qualitative explanation into which the differences of ^{1}H resonance intensity were observed between the presence and absence of suspended clay particles.

Water NOE-driven epitope map of clay–xenobiotic interactions

An epitope map of clay–xenobiotic interactions (Fig. 9) was generated via changes in the NOE build-up rate due to contacts with clay–bound water. The value for the

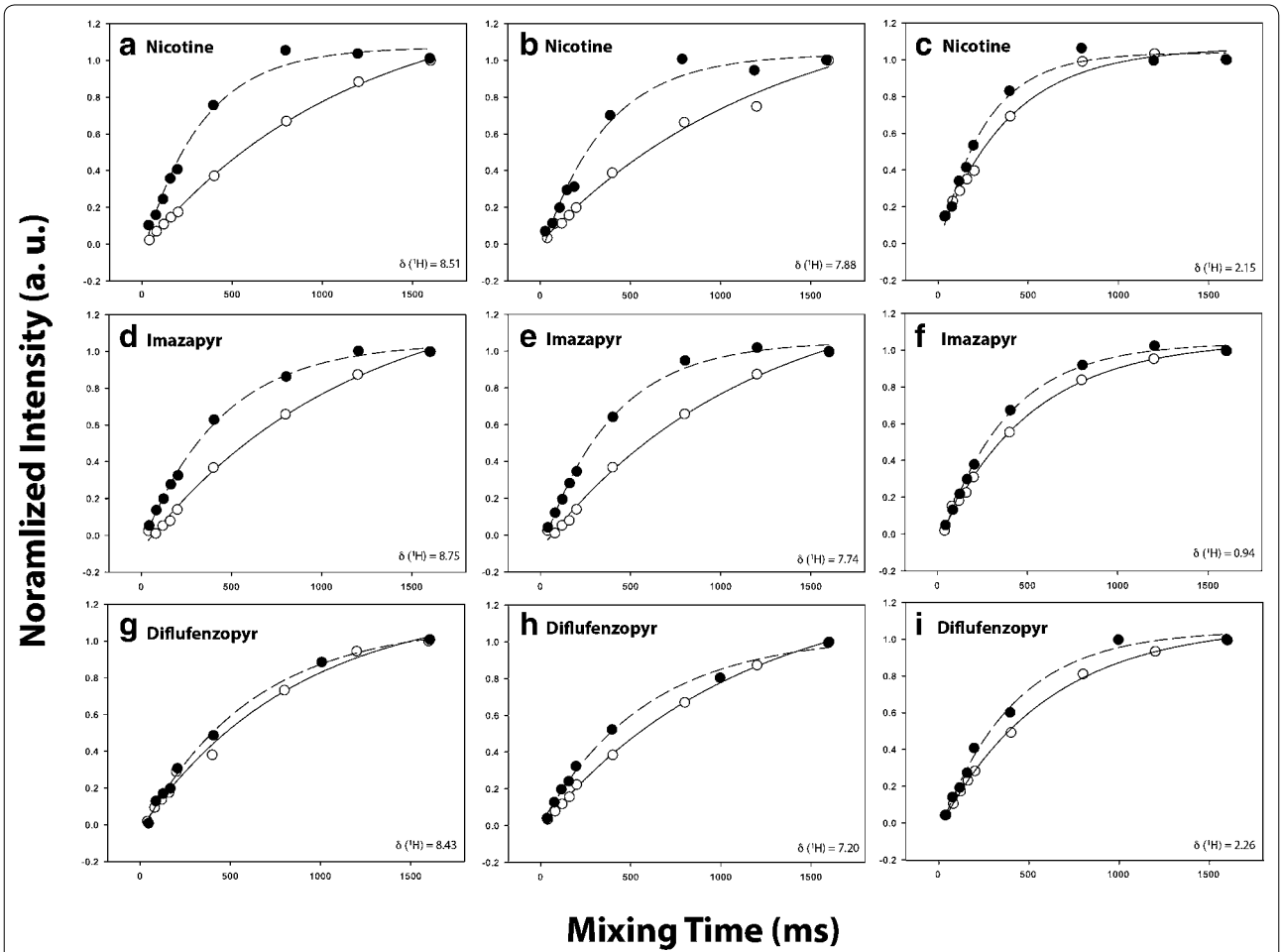

Fig. 7 A series of NOE buildup curves for the various hydrogen resonances in different pesticides. The *filled circle* denotes the NOE buildup in the presence of clay particles, and *open circle* denotes the NOE buildup in the absence of clay. The NOE buildup in the hydrogen of nicotine is shown in Graph (**a**–**c**). The NOE buildup in the hydrogen of imazapyr is shown in Graph (**d**–**f**). The NOE buildup in the hydrogen of Diflufenzopyr is shown in Graph (**g**–**i**). **a**–**c** Nicotine: hydrogen chemical shifts 8.51, 7.88, and 2.15. **d**–**f** Imazapyr: hydrogen chemical shifts 8.75, 7.74, and 0.94. **g**–**i** Diflufenzopyr: hydrogen chemical shifts 8.43, 7.20, and 2.26

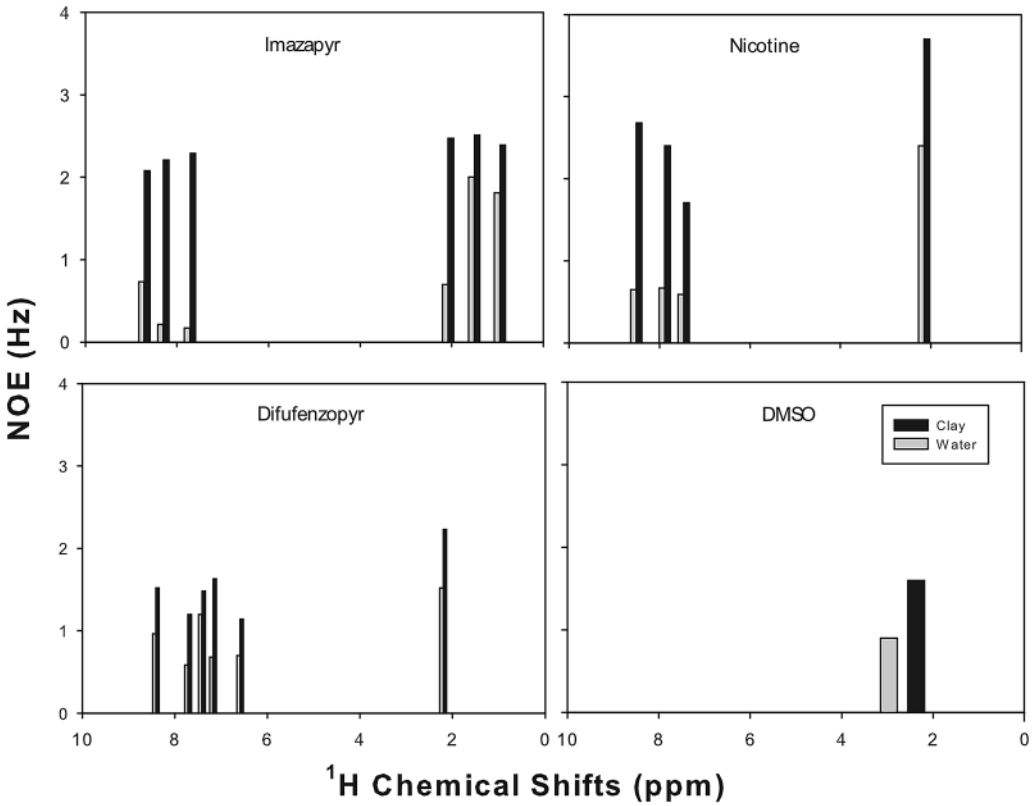

Fig. 8 Bar graphs illustrating the differences in NOE at different ^{1}H chemical shifts in the presence of clay suspension (*black*) and in water (*gray*). In all cases, a general increase in NOE build-up was observed in the presence of clay

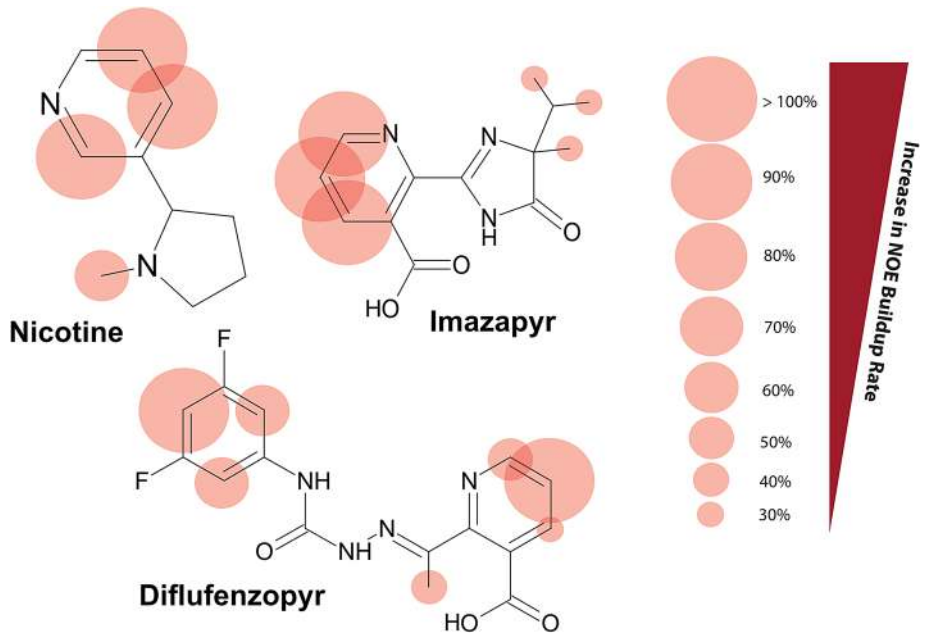

Fig. 9 An epitope map of changes in the water-mediated NOE build-up rate in the presence of suspended clay particles for each of the xenobiotics used in this study Nicotine, Imazapyr, and Diflufenzopyr. Most of the changes in the NOE build-up rate reside in the aromatic region of the molecules

hydrogen peak showing the largest interaction (i.e., largest relative change in presence of clay) is set to 100%, whereas the other hydrogens are progressively scaled accordingly. Such epitope mapping provides an overview of the average molecular orientation of the molecule with respect to the clay. For the case of Nicotine and Imazapyr, most significant changes in the NOE build-up rate were observed in the aromatic moiety. Interestingly, the changes in the NOE build-up rate for aliphatic moieties seem to be moderate as compared to the aromatic counterparts. This can be attributed to a hydrophobic effect, which led to only a moderate change in the water-mediated NOE build-up rate. This was consistent with the literature according to which polycyclic aromatic carbons may bind to clay surfaces [16, 22, 23, 53–55]. In addition, the pyridine moiety, which contains a lone pair of electrons on the nitrogen, is readily available for hydrogen bonding with the water and the hydroxyls groups present on clay surfaces. Therefore, the main contributor to the NOE build-up rate continues to be the close proximity of the hydrogens to the interfacial water.

Furthermore, nitrogen groups, aromatic rings, halogens, and carboxyl group may all represent important contact points with clay, whereas unsubstituted aliphatics appear to have less influence. In addition to calculating the epitope maps from the full NOE build-up curves, it is also possible to calculate maps from a single mixing time, as shown in Fig. 6. Using a single mixing time is advantageous in that only two experiments need to be measured, one in the presence and one in the absence of clay. In turn, this permits molecular binding to be screening in more challenging natural samples or at very low concentration where running multiple experiments across a range of mixing times (i.e. full NOE build-up curves) would be time prohibitive. Figure 10 shows the epitope maps calculated from the data in Fig. 6 collected at a single mixing time. These epitope maps are generally similar to those in Fig. 9 with the main exception of the methyl groups which tend to be over-emphasized in Fig. 10. In Fig. 9, the data are derived from NOE only, which is itself influenced by both exchange and dipolar interactions. Rotational exchange of methyl groups leads to dipolar fluctuations which in turn contribute to NOE. Conversely, the method of calculation used in Fig. 9 is based on cross-relaxation rate (σ) and therefore the interaction itself. In simple terms, a method based on

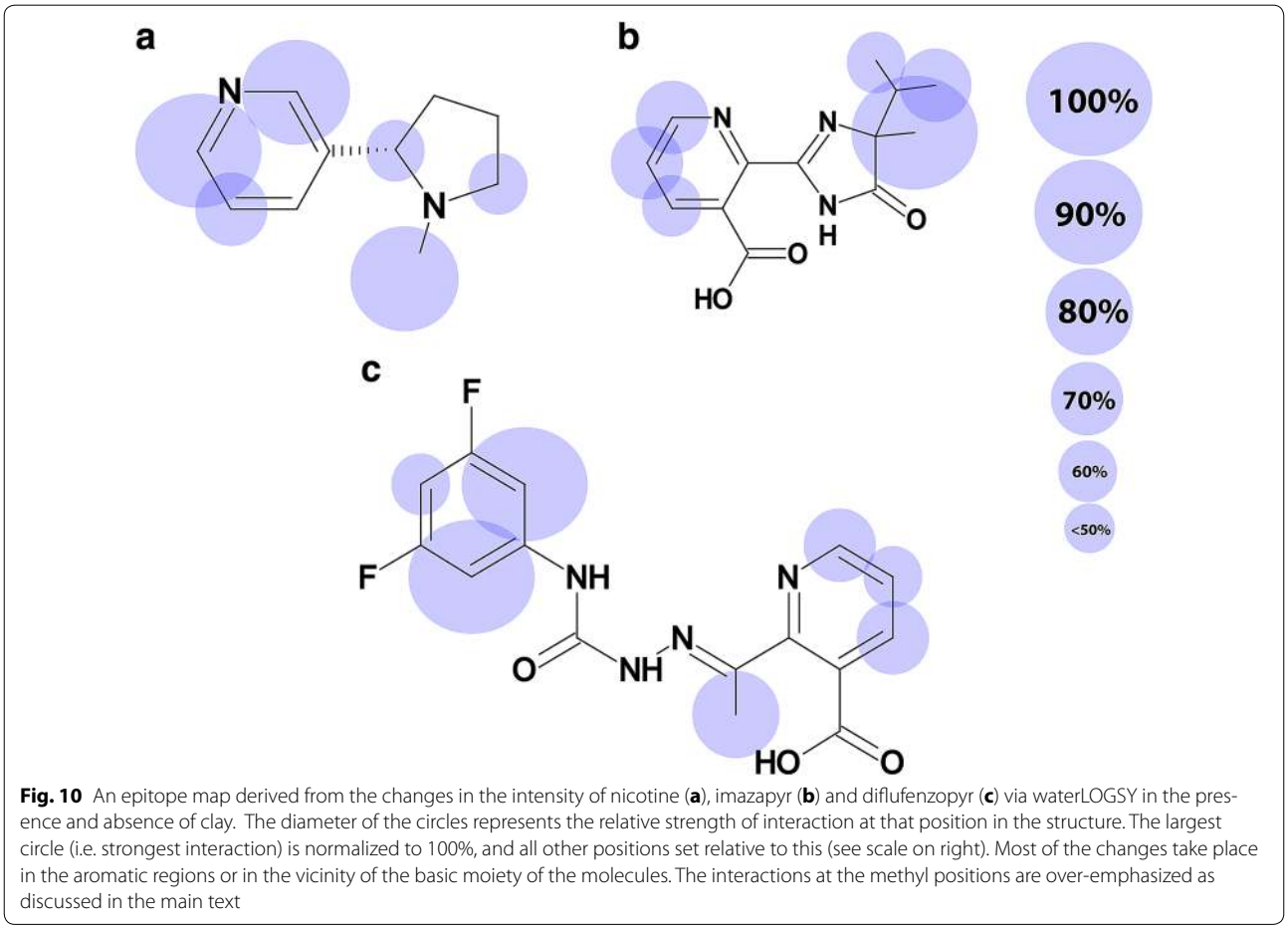

Fig. 10 An epitope map derived from the changes in the intensity of nicotine (**a**), imazapyr (**b**) and diflufenzopyr (**c**) via waterLOGSY in the presence and absence of clay. The diameter of the circles represents the relative strength of interaction at that position in the structure. The largest circle (i.e. strongest interaction) is normalized to 100%, and all other positions set relative to this (see scale on right). Most of the changes take place in the aromatic regions or in the vicinity of the basic moiety of the molecules. The interactions at the methyl positions are over-emphasized as discussed in the main text

cross relaxation derived from a full NOE build-up (i.e. Fig. 9) will give the most accurate mechanism of interactions. Conversely, epitope maps from a single mixing time (Fig. 10) will also provide the dominant mechanism signals, albeit groups with fast rotational exchange may be over-emphasized. However, the fact that the latter method requires only two experiments enables interaction-based studies at low concentration and permits the studies of relatively rapid changes in interactions during processes such as swelling, drying, and remediation.

In summary, NOE-based approaches outlined here should provide a key tool to study the dynamic interactions of organic molecules with mineral surfaces. Further studies using a wider array of structures, different clay, cations, and pH will be needed to fully elucidate the relative influence of functional groups and structural motifs on clay binding. Many of the NMR applications currently present in the literature mainly focus on the irreversible binding of anthropogenic compounds with clay particles. However, the water-mediated NOE approach introduced in this study should represent a further complimentary approach to enable interrogation of systems involving reversible binding in the fast exchange regime. In addition, it allows a better understanding of the role played by interfacial water in the thermodynamics of xenobiotic interactions. Importantly, it has been suggested over the years that this interfacial water, namely vicinal water, provides a favorable environment for organic compounds to partition from bulk aqueous environments [53]. Although none of these models have been verified through high-resolution spectroscopic means, a comprehensive interrogation into these models will provide a better understanding of how clay particles facilitate the partitioning of organics from bulk water environments, which is fundamental to the question of transport, bioavailability, and bioaccessiblity of anthropogenic contaminants and agrochemicals [53].

Conclusion

The water-mediated NOE approach was successfully applied to study the interactions established between several xenobiotics and a model clay. This approach takes advantage of the differences in the NOE build-up rate developing when a compound is in contact with the clay vicinal water, which leads to a change in the sign of NOE. The latter effect manifests itself only when the molecule resides on clay surfaces for longer than 2 ns. Therefore, this is a tool to screen compounds as a function of their affinity with clay. Importantly, the sorption of anthropogenic compounds on clay minerals is a complex multivariable problem with intricate interacting parameters that warrant an in-depth investigation. The water-mediated NOE approach can provide insights into the role that vicinal water played in the binding process whether it is kinetically or thermodynamically driven. Therefore, this further validates the incorporation of this approach in the current repertoire of NMR experiments used in organo-mineral research.

Abbreviations

NMR: nuclear magnetic resonance; NOE: nuclear overhauser effect; SOM: soluble organic matters; SANS: small-angle neutrons scattering; XRD: x-ray powder diffraction; CMP: comprehensive multiphase; STD: saturation transfer difference; SSNMR: solid-state NMR; CP-MAS: cross polarization magic angle spinning; WaterLOGSY: Water Ligand Observed via Gradient Spectroscopy; r.f.: radio frequency; DMSO: dimethyl sulfoxide.

Authors' contributions

RS carried out the experiments and drafted the manuscript. AB assisted in carrying out the experiments and JW prepared the clay particles. HF and DCM assisted in drafting the manuscript. AJS conceived this study and drafted the manuscript. All authors read and approved the final manuscript.

Acknowledgements

AJS thanks NSERC, (Strategic and Discovery Programs), the Canada Foundation for Innovation (CFI), the Ministry of Research and Innovation (MRI), and Krembil Foundation for providing funding. AJS also thanks the Government of Ontario for an Early Researcher Award. AJS would like to thank Dr. Rudraksha Dutta Majumdar for reading the manuscripts and his helpful suggestions.

Competing interests

The authors declare that they have no competing interests.

Consent of publication

The publisher has our consent to publish this manuscript including figures and associated data.

Funding

This study is supported by Grants from NSERC (Strategic and Discovery Programs), the Canadian Foundation for innovation (CFI), the Ministry of Research and Innovation (MRI), and Krembil Foundation.

Received: 31 August 2016 Accepted: 3 December 2016
Published online: 25 January 2017

References

1. Staples CA, Dorn PB, et al. A review of the environmental fate, effects, and exposures of bisphenol A. Chemosphere. 1998;36(10):2149–73.
2. Erbe MC, Ramsdorf WA, et al. Toxicity evaluation of water samples collected near a hospital waste landfill through bioassays of genotoxicity piscine micronucleus test and comet assay in fish astyanax and ecotoxicity *Vibrio fischeri* and *Daphnia magna*. Ecotoxicology. 2011;20(2):320–8.
3. Milla S, Depiereux S, et al. The effects of estrogenic and androgenic endocrine disruptors on the immune system of fish: a review. Ecotoxicology. 2011;20(2):305–19.
4. Kidd KA, Blanchfield PJ, et al. Collapse of a fish population after exposure to a synthetic estrogen. Proc Natl Acad Sci USA. 2007;104(21):8897–901.
5. Weinberger B, Vetrano AM, et al. Effects of maternal exposure to phthalates and bisphenol a during pregnancy on gestational age. J Matern Fetal Neonatal Med. 2014;27(4):323–7.
6. Zeman FA, Boudet C, et al. Exposure assessment of phthalates in French pregnant women: results of the ELFE pilot study. Int J Hyg Environ Health. 2013;216(3):271–9.
7. Yuk J, McKelvie JR, et al. Comparison of 1-d and 2-d nmr techniques for screening earthworm responses to sub-lethal endosulfan exposure. Environ Chem. 2010;7(6):524–36.

8. Yuk J, Simpson MJ, et al. 1-d and 2-d NMR metabolomics of earthworm responses to sub-lethal trifluralin and endosulfan exposure. Environ Chem. 2011;8(3):281–94.
9. Yuk J, Simpson MJ, et al. 1-d and 2-d NMR-based metabolomics of earthworms exposed to endosulfan and endosulfan sulfate in soil. Environ Pollut. 2013;175:35–44.
10. Lankadurai BP, Simpson AJ, et al. H-1 NMR metabolomics of *Eisenia fetida* responses after sub-lethal exposure to perfluorooctanoic acid and perfluorooctane sulfonate. Environ Chem. 2012;9(6):502–11.
11. Lankadurai BP, Wolfe DM, et al. H-1 NMR-based metabolomic observation of a two-phased toxic mode of action in *Eisenia fetida* after sub-lethal phenanthrene exposure. Environ Chem. 2011;8(2):105–14.
12. Shirzadi A, Simpson MJ, et al. Molecular interactions of pesticides at the soil–water interface. Environ Sci Technol. 2008;42(15):5514–20.
13. Shirzadi A, Simpson MJ, et al. Application of saturation transfer double difference nmr to elucidate the mechanistic interactions of pesticides with humic acid. Environ Sci Technol. 2008;42(4):1084–90.
14. Longstaffe JG, Courtier-Murias D, et al. The ph-dependence of organofluorine binding domain preference in dissolved humic acid. Chemosphere. 2013;90(2):270–5.
15. Simpson MJ, Simpson AJ. The chemical ecology of soil organic matter molecular constituents. J Chem Ecol. 2012;38(6):768–84.
16. Meleshyn A, Tunega D. Adsorption of phenanthrene on Na-montmorillonite: a model study. Geoderma. 2011;169:41–6.
17. De Stefanis A, Tomlinson AAG, et al. Nanostructures of the montmorillonite-derived restructured clays K10 (r), HMO and the Mg^{2+} exchanged analogue Mg-HMO. ASANS, N_2 sorption and XRPD study. J Mater Chem. 2003;13(5):1145–8.
18. Delville A. Modeling the clay water interface. Langmuir. 1991;7(3):547–55.
19. Takeda M, Matsunaga T, et al. Rheo-SANS studies on shear thickening in clay-poly(ethylene oxide) mixed solutions. Macromolecules. 2010;43(18):7793–9.
20. Kelleher BP, Simpson AJ. Humic substances in soils: are they really chemically distinct? Environ Sci Technol. 2006;40(15):4605–11.
21. Simpson AJ, Simpson MJ, et al. The application of ^{1}H high-resolution magic-angle spinning NMR for the study of clay–organic associations in natural and synthetic complexes. Langmuir. 2006;22(10):4498–503.
22. Schlautman MA, Morgan JJ. Sorption of perylene on a nonporous inorganic silica surface-effects of aqueous chemistry on sorption rates. Environ Sci Technol. 1994;28(12):2184–90.
23. Schwarzenbach RP, Westall J. Transport of non-polar organic-compounds from surface-water to groundwater—laboratory sorption studies. Environ Sci Technol. 1981;15(11):1360–7.
24. Malwitz MM, Butler PD, et al. Orientation and relaxation of polymer-clay solutions studied by rheology and small-angle neutron scattering. J Polym Sci B Polym Phys. 2004;42(17):3102–12.
25. Simpson AJ, Simpson MJ, et al. Nuclear magnetic resonance spectroscopy and its key role in environmental research. Environ Sci Technol. 2012;46(21):11488–96.
26. Farooq H, Courtier-Murias D, et al. HR-MAS NMR spectroscopy: a practical guide for natural samples. Curr Org Chem. 2013;17(24):3013–31.
27. Clemente JS, Gregorich EG, et al. Comparison of nuclear magnetic resonance methods for the analysis of organic matter composition from soil density and particle fractions. Environ Chem. 2012;9(1):97–107.
28. Mazzei P, Piccolo A. Interactions between natural organic matter and organic pollutants as revealed by NMR spectroscopy. Magn Reson Chem. 2015;53(9):667–78.
29. Tadini AM, Constantino IC, et al. Characterization of typical aquatic humic substances in areas of sugarcane cultivation in brazil using tetramethylammonium hydroxide thermochemolysis. Sci Total Environ. 2015;518–519:201–8.
30. Tadini AM, Pantano G, et al. Off-line TMAH-GC/MS and NMR characterization of humic substances extracted from river sediments of northwestern sao paulo under different soil uses. Sci Total Environ. 2015;506–507:234–40.
31. Shirzadi A, Simpson MJ, et al. Application of saturation transfer double difference NMR to elucidate the mechanistic interactions of pesticides with humic acid. Environ Sci Technol. 2008;42(4):1084–90.
32. Simpson AJ, Simpson MJ, et al. Nuclear magnetic resonance spectroscopy and its key role in environmental research. Environ Sci Technol. 2012;46(21):11488–96.
33. Nebbioso A, Piccolo A. Advances in humeomics: enhanced structural identification of humic molecules after size fractionation of a soil humic acid. Anal Chim Acta. 2012;720:77–90.
34. Nebbioso A, Piccolo A. Molecular characterization of dissolved organic matter (DOM): a critical review. Anal Bioanal Chem. 2013;405(1):109–24.
35. Mazzei P, Piccolo A. Quantitative evaluation of noncovalent interactions between glyphosate and dissolved humic substances by NMR spectroscopy. Environ Sci Technol. 2012;46(11):5939–46.
36. Masoom H, Courtier-Murias D, et al. From spill to sequestration: the molecular journey of contamination via comprehensive multiphase NMR. Environ Sci Technol. 2015;49(24):13983–91.
37. Wheeler HL, Soong R, et al. Comprehensive multiphase NMR: a promising technology to study plants in their native state. Magn Reson Chem. 2015;53(9):735–44.
38. Courtier-Murias D, Farooq H, et al. Comprehensive multiphase nmr spectroscopy: basic experimental approaches to differentiate phases in heterogeneous samples. J Magn Reson. 2012;217:61–76.
39. Longstaffe JG, Simpson MJ, et al. Identifying components in dissolved humic acid that bind organofluorine contaminants using $^{1}H\{^{19}F\}$ reverse heteronuclear saturation transfer difference NMR spectroscopy. Environ Sci Technol. 2010;44(14):5476–82.
40. Dalvit C, Fogliatto G, et al. WaterLOGSY as a method for primary NMR screening: practical aspects and range of applicability. J Biomol NMR. 2001;21(4):349–59.
41. Dalvit C, Pevarello P, et al. Identification of compounds with binding affinity to proteins via magnetization transfer from bulk water. J Biomol NMR. 2000;18(1):65–8.
42. Sanders RL, Mueller KT. Investigating clay mineral surface reactivity across scales using solid-state nuclear magnetic resonance. Geochim Cosmochim Acta. 2009;73(13):A1153-A.
43. Sanders RL, Washton NM, et al. Measurement of the reactive surface area of clay minerals using solid-state NMR studies of a probe molecule. J Phys Chem C. 2010;114(12):5491–8.
44. Sanders RL, Washton NM, et al. Atomic-level studies of the depletion in reactive sites during clay mineral dissolution. Geochim Cosmochim Acta. 2012;92:100–16.
45. Delville A, Grandjean J, et al. Order acquisition by clay platelets in a magnetic-field-NMR-study of the structure and microdynamics of the adsorbed water layer. J Phys Chem. 1991;95(3):1383–92.
46. Antanasijevic A, Ramirez B, et al. Comparison of the sensitivities of water-LOGSY and saturation transfer difference NMR experiments. J Biomol NMR. 2014;60(1):37–44.
47. Gossert AD, Henry C, et al. Time efficient detection of protein–ligand interactions with the polarization optimized PO-waterlogsy NMR experiment. J Biomol NMR. 2009;43(4):211–7.
48. Sun P, Jiang X, et al. Biomolecular ligands screening using radiation damping difference waterLOGSY spectroscopy. J Biomol NMR. 2013;56(3):285–90.
49. Balbach J, Forge V, et al. Detection of residue contacts in a protein folding intermediate. Proc Natl Acad Sci USA. 1997;94(14):7182–5.
50. Sposito G, Prost R. Structure of water adsorbed on smectites. Chem Rev. 1982;82(6):553–73.
51. Booker CJ, Bedmutha R, et al. Experimental investigations into the insecticidal, fungicidal, and bactericidal properties of pyrolysis bio-oil from tobacco leaves using a fluidized bed pilot plant. Ind Eng Chem Res. 2010;49(20):10074–9.
52. Olejnik S, Aylmore AG, et al. Infrared spectra of kaolin mineral-dimethyl sulfoxide complexes. J Phys Chem. 1968;72(1):241–9.
53. Zhu DQ, Herbert BE, et al. Cation-pi bonding: a new perspective on the sorption of polycyclic aromatic hydrocarbons to mineral surfaces. J Environ Qual. 2004;33(4):1322–30.
54. Solc R, Gerzabek MH, et al. Wettability of kaolinite (001) surfaces—molecular dynamic study. Geoderma. 2011;169:47–54.
55. Hur J, Schlautman MA. Influence of humic substance adsorptive fractionation on pyrene partitioning to dissolved and mineral-associated humic substances. Environ Sci Technol. 2004;38(22):5871–7.